A quantitative comparison of in-line coating thickness distributions obtained from a pharmaceutical tablet mixing process using discrete element method and terahertz pulsed imaging

Chunlei Pei[1], Hungyen Lin[2,3], Daniel Markl[3], Yao-Chun Shen[4], J. Axel Zeitler[3] and James A. Elliott[1*]

[1]Department of Materials Science and Metallurgy, 27 Charles Babbage Road, University of Cambridge, CB3 0FS, UK

[2]Department of Engineering, Lancaster University, Lancaster LA1 4YW, UK

[3]Department of Chemical Engineering and Biotechnology, University of Cambridge, Cambridge CB2 0AS, UK

[4]Department of Electrical Engineering and Electronics, University of Liverpool, Liverpool L69 3GJ, UK

[*] Corresponding author. Tel.: +44 1223 335987; fax: +44 1223 334567.
E-mail address: jae1001@cam.ac.uk

Abstract

The application of terahertz pulsed imaging (TPI) in the in-line configuration to monitor the coating thickness distribution of pharmaceutical tablets has the potential to improve the performance and quality of the spray coating process. In this study, an in-line TPI method is used to measure coating thickness distributions on pre-coated tablets during mixing in a rotating pan, and compared with results obtained numerically using the discrete element method (DEM) combined with a ray-tracing technique. The hit rates (i.e. the number of successful coating thickness measurements per minute) obtained from both terahertz in-line experiments and the DEM/ray-tracing simulations are in good agreement, and both increase with the number of baffles in the mixing pan. We demonstrate that the coating thickness variability as determined from the ray-traced data and the terahertz in-line measurements represents mainly the intra-tablet variability due to relatively uniform mean coating thickness across tablets. The mean coating thickness of the ray-traced data from the numerical simulations agrees well with the mean coating thickness as determined by the off-line TPI measurements. The mean coating thickness of in-line TPI measurements is slightly higher than that of off-line measurements. This discrepancy can be corrected based on the cap-to-band surface area ratio of the tablet and the cap-to-band sampling ratio obtained from ray-tracing simulations: the corrected mean coating thickness of the in-line TPI measurements shows a better agreement with that of off-line measurements.

Keywords: terahertz in-line sensing; terahertz pulsed imaging; coating thickness variability; discrete element method; pharmaceutical coating

1. Introduction

Pharmaceutical tablets are commonly coated with one or multiple polymeric film layers for cosmetic and functional purposes (Ho et al., 2007; Turton, 2008). The tablet coating process is typically performed inside a rotating pan coater in order to facilitate good mixing of the tablets. The final coating thickness distribution is critical in determining the quality of the process and final products (Brock et al., 2013a, 2013b; Freireich et al., 2015; Ketterhagen, 2011). In order to monitor and control the manufacturing process, a non-destructive in-line sensing method can be desirable to provide real-time feedback information on the coating thickness of tablets. Various in-line techniques have been developed to measure the coating thickness, including near-infrared (NIR) spectroscopy (Moes et al., 2008; Möltgen et al., 2012; Pérez-Ramos et al., 2005), Raman spectroscopy (Wirges et al., 2013), optical coherence tomography (OCT) (Markl et al., 2015), terahertz pulsed imaging (TPI) (May et al., 2011) and more recently, a combination of TPI and OCT (Lin et al., 2017).

In-line sensing with TPI has the advantage that it is a calibration-free method, apart from having to measure the refractive index of the coating material (Haaser et al., 2013; Lin et al., 2015b; Shen, 2011). In contrast, NIR and Raman spectroscopies typically measure the coating thickness indirectly by using a multivariate model, which relates the measured amplitude of spectral features originating from a coating or a core constituent to a reference measurement (e.g. coating thickness). Both methods rely on calibration models to relate the measured features to the coating thickness prior to the in-line measurement. X-ray computed tomography is another technique that has been used to quantify the absolute coating thickness yielding a full high-resolution 3D map of the tablet, which in turn could be used to calculate the refractive indices at terahertz or optical frequencies (Lin et al., 2017). However, TPI is fundamentally different from the spectroscopic

methods as it provides depth-resolved information to directly measure the coating thickness. In this latter technique, a terahertz pulse is focused on the surface of the tablet, where a substantial part of the radiation is reflected. However, a fraction of the terahertz radiation penetrates the polymeric material and is then reflected at the interface between the coating layer and the tablet core due to the difference in refractive indices between these two media. The time difference between the two reflected pulses is measured and used to determine the thickness of the coating layer, knowing the refractive index of the coating material. In-line sensing with terahertz radiation has been used previously to monitor the tablet pan coating process (May et al., 2011). In that work, a terahertz sensor was positioned at the side of the rotating pan coater in order to focus terahertz pulses onto the inner surface of the perforated pan. The terahertz pulse was either reflected by the metallic pan, or passed through the perforations and reflected back by a tablet to the receiver lens. The average coating thickness obtained from this terahertz in-line method agreed well with off-line measurements from all pixels of the TPI coating maps generated over the entire surface of 20-30 tablets (May et al., 2011). The work also revealed a comparable thickness distribution to off-line measurements with a slightly larger variance, which indicates that the in-line method can measure the coating thickness distribution within the tablet bed during the coating process.

However, a single terahertz in-line measurement only originates from a single spot on a tablet within the coating pan. Under normal process conditions, it is generally not possible to determine the particular tablet and the precise spot on that tablet from which the measurement was taken. Therefore, it is not straightforward to establish whether the coating thickness distribution from the terahertz in-line method corresponds to either inter- or intra-tablet coating thickness distribution, or indeed a mixture of the two. Such knowledge would be very useful for assessing the coating quality and developing deeper process understanding. In order to determine what type of coating

thickness distribution is represented by the terahertz in-line measurements, the location where the terahertz beam hits on the tablet must be identified more precisely. To fulfil this purpose experimentally, OCT was recently implemented into an in-line system together with TPI to monitor the spray coating of tablets in a coating pan (Lin et al., 2017). Due to a much higher sampling frequency, OCT can measure the coating thickness along a line on the surface of the sample as opposed to only a single point on each tablet. Given the known geometry of the tablets in the coating pan, this information provides some indication of the location of the measurement spot on the surface of the tablet. However, as we have recently demonstrated (Lin et al., 2017), OCT measurements can be compromised by scattering from pigmentation particles in the coating material. The method is only able to measure relatively thin coatings reliably (e.g. < 80 μm). The longer wavelength of terahertz radiation compared to that of near-infrared light as used in OCT instruments renders TPI more suitable to assess thick coatings layers (Lin et al., 2015a).

Analytical and numerical modelling methods (Freireich and Wassgren, 2010; Toschkoff et al., 2013, 2015; Freireich et al., 2015; Boehling et al., 2016; Pei and Elliott, 2017), using the discrete element method (DEM), have recently been employed to investigate inter- and intra-tablet variability during the coating process. Freireich et al. (2015) used glued spheres (multi-spheres) to model the shape of the tablet and calculated the dynamics of tablets in a rotating pan. The positions and orientations of multi-spheres from each DEM simulation were mapped onto the tablets of which surfaces were meshed into triangular elements. Each of these triangular elements was indexed with a specific colour and visualised on a 2-D image which is a projection following the spray direction. Based on the position and colour of each pixel in the image, and whether the corresponding triangular element is in the specified spray area within each frame of the DEM simulation, the coating mass transfer is simulated by adding a uniform amount of coating to each

triangular element. The intra- and inter-tablet coating thickness distributions can then be analysed based on the values of the coating thickness on each triangular element. Using this image analysis method, the overlap between triangular elements with respect to the spray direction (shadow effect/depth test) can be considered. Therefore, each pixel in this method essentially represents a ray following the spray direction from the spray nozzle to the tablet surface. This method ensures that mass transfer is only applied to surface elements of the tablet that are not obstructed by other tablets in the tablet bed of the coater. The ray-tracing method can also be explicitly implemented to represent trajectories of discrete spray droplets (Toschkoff et al., 2015, 2013; Pei and Elliott, 2017). In this method, the spray droplets are allowed to accumulate on the tablet surface where the locations of accumulations are the intersection points calculated from the direction of the ray and the position of the tablet. On the other hand, with the growing interest of in-line measurement for process understanding and control, the explicit ray tracing method based on these intersection points can provide detailed coating thickness information from coated tablets for comparison against experimental measurements.

In this paper, the coating thickness of film-coated tablets mixing in a laboratory scale perforated coating pan is measured using the terahertz in-line method. In order to obtain and analyse the relationship between in-line measurements and intra- and inter-tablet coating thickness distributions, DEM and ray-tracing methods are implemented to model the mixing and terahertz in-line sampling processes. The hit rates and coating thickness distributions from the terahertz in-line measurements are analysed and compared with the numerical analysis and off-line measurements.

2. Methodology

2.1 Experimental coating thickness measurements

The coated tablets were prepared in a side-vented pan coater (BFC5, L.B. Bohle, Germany) using biconvex placebo cores (tablet radius 4 mm, radius of curvature 9 mm, centre thickness 4 mm). The tablet weighed 222.1 mg in average with a standard deviation of 4.0 mg. The coating formulation consisted of 75% Walocel HM5 PA2910 (Hypromellose, Wolff Cellulosics, Germany) and 25% polyethylene glycol 1500 (wt % solids).

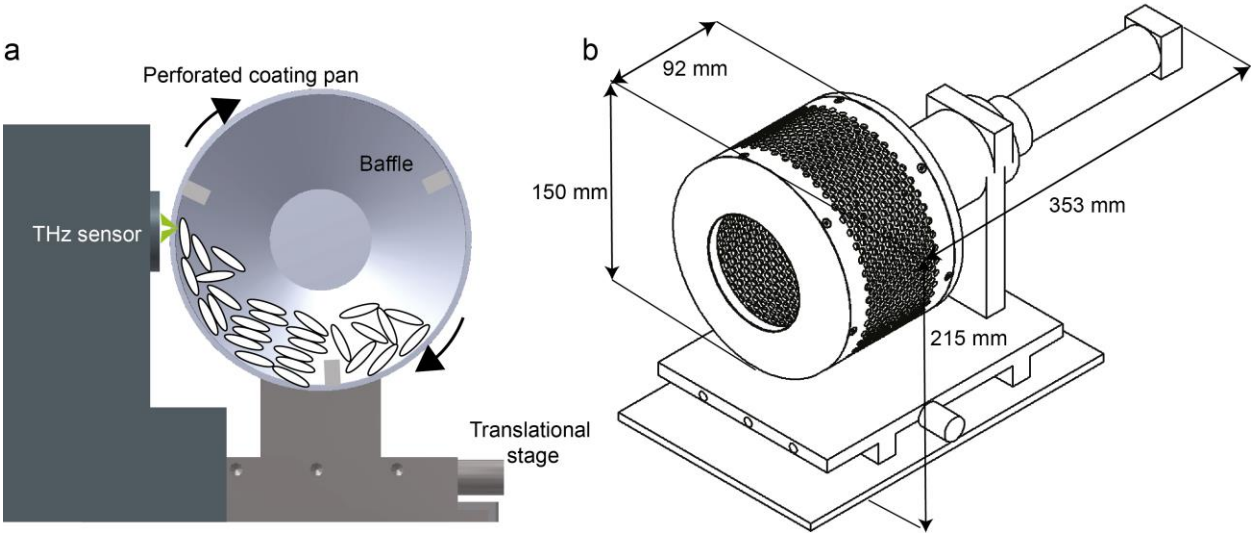

Figure 1: The experimental setup: (a) a laboratory scale pan coater coupled to the TPI sensor for in-line sensing, and (b) a schematic of the pan coater in perspective view.

The experimental measurements were divided into 2 sets: off-line and in-line. In the off-line measurement, the coating thickness maps covering the surfaces of 24 coated tablets were measured by TPI for the comparison with the terahertz in-line measurement. A TPI Imaga 2000 system

(TeraView Ltd., Cambridge, UK) was used to perform the off-line measurements as described in detail by Shen and Taday (2008). During the measurement, each tablet was scanned using a six-axis robot system to ensure that the terahertz beam was in focus and perpendicular to the tablet surface. Mapping of the whole tablet surface was performed using a point-to-point scan at a lateral resolution of 200 μm. The coating thickness, *h*, was calculated as:

$$h = \frac{\Delta t\, c}{2n} \tag{1}$$

where Δt is the time-of-flight from the tablet surface to the coating interface; c is the speed of light in vacuum; and n is the refractive index of the coating material, which is taken as 1.5 in this study (Russe et al., 2012) for the coating formulation as described above at the terahertz frequencies.

In the in-line measurement, 50 g of coated tablets (approximately 230 in number) were loaded into a bespoke lab-scale coating pan that was designed and commissioned for terahertz in-line measurement as shown in Figure 1 (Lin et al., 2017). Since the terahertz sensor is fixed in the TPI Imaga 2000, the coating pan was designed to fit inside the enclosure of the TPI Imaga 2000 system, where the terahertz sensor was located perpendicular to the centre of the coating pan. The perforated coating pan had a wall thickness of 2 mm and an overall diameter (D_d) of 150 mm while each circular perforation had a diameter of 4.2 mm. Perforation patterning resulted in a 45% opening of the external surface of the pan.

The 1.2 litre coating pan was additionally fitted with 1, 3 and 6 drive bars (baffles) to facilitate the mixing of the tablet bed. It should be noted that the simple tubular baffle design used in this study does not realistically reflect the complex designs used in the pharmaceutical industry. They are primarily used to lift the tablets up to the measurement position and increase the frequency of

measurement for comparison with DEM. Each baffle has a length of 70 mm corresponding to the longitudinal axis of the coating pan, a thickness of 6.2 mm and a width of 8 mm towards the centre of the coating pan.

The rotational movement of the coater was driven by an A-max 32 permanent magnet DC motor with a closed loop speed control (Maxon Motor AG, Switzerland) at 15 rpm. To ensure that the generated terahertz pulses were focused onto the surface of tablets inside the coating pan, the sensor was kept at a fixed distance that matched the 7 mm focal length of the terahertz sensor optics from the inner wall of the coating pan. Taking into account the distance of travel on the mesh and the tablet tangential speed, reflected terahertz time-domain waveforms were recorded at a rate of 30 Hz (acquisition time of a single waveform was 33.3 ms) with no signal averaging to ensure that the likelihood of multiple measurements on a single tablet is minimised. Each experiment was limited to 10 minutes in duration so as to reduce the amount of attrition of the coated tablets. The terahertz beam was incident on the tablet surface at an angle of 30 °. The acquired measurements were saved and processed off-line (Matlab R2015b; The MathWorks Inc., Natick, MA) using the previously presented analysis algorithm (May et al. 2010, Lin et al. 2015b) with the settings for the selection criteria determined based on the off-line analysis of the coated tablets. In this study, we performed only mixing of film-coated tablets, while the in-line measurement of tablet coating process using TPI and OCT was recently demonstrated using the same equipment by Lin et al. (2017).

2.2 Numerical model of in-line measurement

The numerical study is divided into two stages. In the first stage, the dynamics of tablets during mixing was modelled using Discrete Element Method (DEM) simulations, and in the second stage, as a post-processing step, a ray-tracing method (Toschkoff et al., 2015, 2013; Pei and Elliott, 2017)

was applied to the outputs of DEM simulations to trace the trajectory of the terahertz ray and detect its intersection with the tablet.

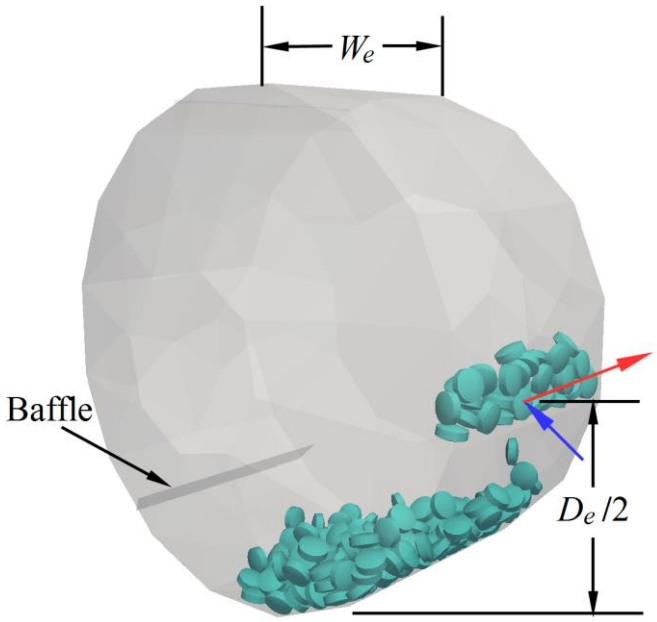

Figure 2: DEM and ray-tracing setup. The geometry of the pan is 75 mm in width (We) and 146 mm in diameter (De) which are corresponding to the internal surface of the coating pan in experiments. Meshed tablets using the position and orientation of multi-spheres from DEM simulations are used for the ray-tracing process. The (terahertz) ray is positioned at the half height of the pan, De/2 (i.e. Dd/2). The incoming ray is from an oblique direction at an incident angle of 30°. A 'hit' is representative of a detection from the reflected ray.

DEM simulations were employed to model the mixing behaviour of tablets in a rotating pan as shown in Figure 2. The shape of the tablet in DEM was approximated using the multi-sphere method to ensure the effects of the tablet shape on the dynamics of tablets during mixing were

accounted for (Pei et al., 2015). The pan was discretised into 332 triangular elements while the 3D model of the tablet from the experiment was meshed into triangles and then 14 constituent spheres were used to approximately mimic the shape of the meshed tablet as shown in Figure 3. The choice for the number of triangular elements for the pan and for constituent spheres for the tablet was based on a trade-off between faithfully representing the shape and mechanics of the objects while minimising the computational time. The open source software package LIGGGHTS 3.1.0 (Kloss et al., 2012) was used to compute the dynamics of the multi-sphere objects (tablets) in the mixing process. The contact between constituent spheres from different tablets was calculated based on the Hertz-Mindlin contact model (Di Renzo and Di Maio, 2004). The multi-spheres were treated as rigid bodies that follow Newton's second law of motion using a quaternion rigid body algorithm.

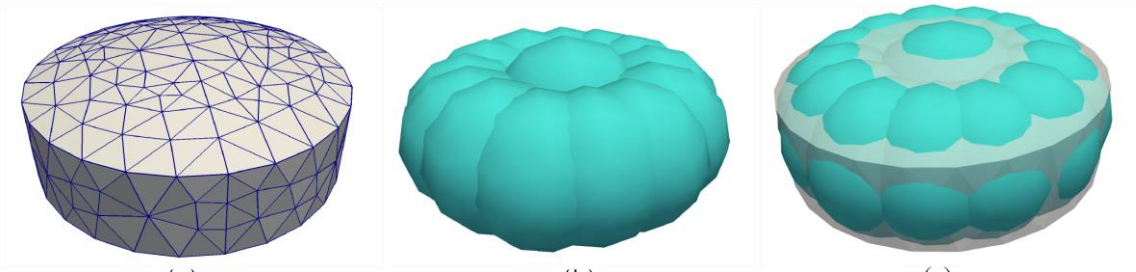

Figure 3: Meshed and multi-sphere tablets: (a) meshed tablets; (b) multi-sphere tablet; (c) overlapped meshed and multi-sphere tablets. The multi-sphere tablet is used in DEM simulations while the meshed tablet is used in the ray-tracing process.

Table 1: Material properties and process conditions

Parameters	Values
Tablet density	1300 kg m^{-3}
Tablet mass	~ 220 mg
Tablet Young's modulus	5.0 GPa
Tablet Poisson's ratio	0.3
Pan density	7800 kg m^{-3}
Pan Young's modulus	210 GPa
Pan Poisson's ratio	0.3
Coefficient of friction (tablet-tablet)	0.5
Coefficient of friction (tablet-pan)	0.5
Coefficient of restitution	0.74
Total simulated mixing time	~ 5 mins
Time interval for export	0.033 s

In the simulation, 230 multi-sphere tablets with a total mass of 50 g were deposited into the pan and mixed as the pan rotates at 15 rpm. The positions and quaternion orientations of multi-spheres were exported at every 0.033 s corresponding to the 30 Hz sampling frequency of terahertz measurement, and then mapped onto the meshed tablets for further ray-tracing analysis. 1, 3 and 6 baffles were used respectively to investigate the effect of baffles on the mixing process. Further to the geometrical dimensions of tablets and the pan, other properties of the tablet and pan used as

part of the simulation are listed in Table 1. The interaction parameters, especially the coefficient of friction, vary with the material type as reported by previous experimental studies (Hancock et al., 2010; Suzzi et al., 2012). Hancock et al. (2010) suggested that the tablet-polymer/steel friction coefficient varies from 0.0 to 0.74 according to the material and surface properties while Suzzi et al. (2012) showed that the coefficient of restitution between tablets and marble plate is 0.74 with a standard deviation of 0.03. As the coating pan is equipped with baffles, the influence of coefficient of friction is relatively minor, and was set to 0.5 for all simulations.

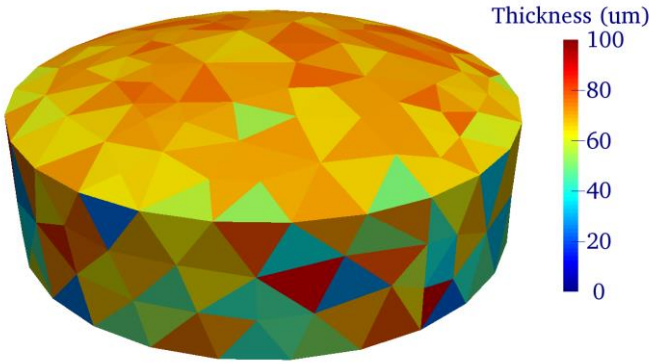

Figure 4: The coating thickness map on an example tablet acquired from the off-line TPI measurement.

The off-line coating thickness of an example tablet measured from TPI was mapped onto a meshed tablet using a triangulation-based nearest neighbour interpolation method (Matlab R2017, The Mathworks Inc., Natick, MA) as shown in Figure 4. Based on the data from the 24 off-line measured tablets, 24 coating maps were projected onto the tablet mesh developed for the ray-

tracing simulation, and the 24 coating thickness maps were uniformly distributed across the 230 tablets.

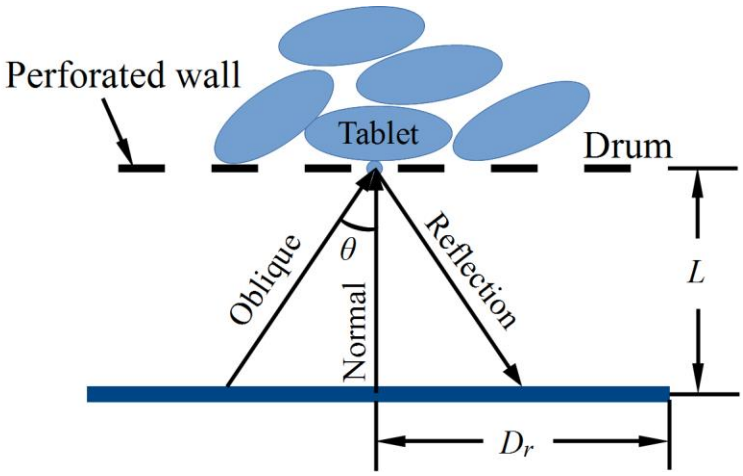

Figure 5: Ray-tracing modes. Both normal and oblique modes are direct detection of the intersection between the ray and tablet, while the reflection mode considers whether the reflected ray can hit the receiver lens.

After DEM simulation, the ray-tracing method was used to sample the coating thickness of tablets in the rotating pan and the numerically sampled data were compared with the in-line TPI measurements. In order to model the trajectory of the terahertz beam, three ray-tracing approaches, including normal, oblique and reflection modes, were introduced as shown in Figure 5. The normal incoming ray was set to be perpendicular to the pan while the oblique incoming ray exhibited an angle of incidence, θ, with respect to the normal direction. For these two modes, the tracing process was ended if the incoming ray did not result in any intersection with any triangle on any tablet. In reflection mode, the incoming ray was incident at an ‘oblique’ direction. When the incoming ray

had an intersection point with a triangle on a tablet, the ray was reflected based on the orientation (normal direction) of the intersected triangle.

A hit with respect to each mode was recorded when the normal distance between the probe and the intersection point is in the range of 7 to 10 mm, loosely corresponding the focal length of TPI (see Appendix A). In the case of reflection mode, the reflected ray must additionally reflect back to the receiver lens within the diameter of D_r (= 8 mm) without being obstructed by another tablet. The recorded hits on the tablets in turn correspond to the thickness values of the intersected triangles. Therefore, the coating thickness distribution from the ray-tracing method can be further used to analyse the inter- and intra-tablet variability based on their locations and compare with the terahertz in-line measurements.

3. Results and discussion

3.1 Comparison of hit rates between simulations and in-line experiments

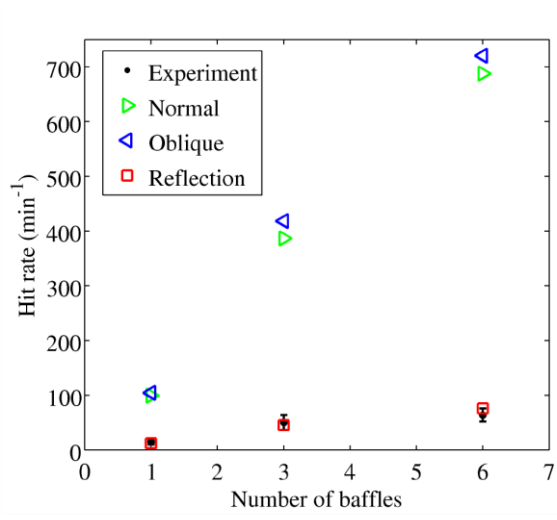

(a)

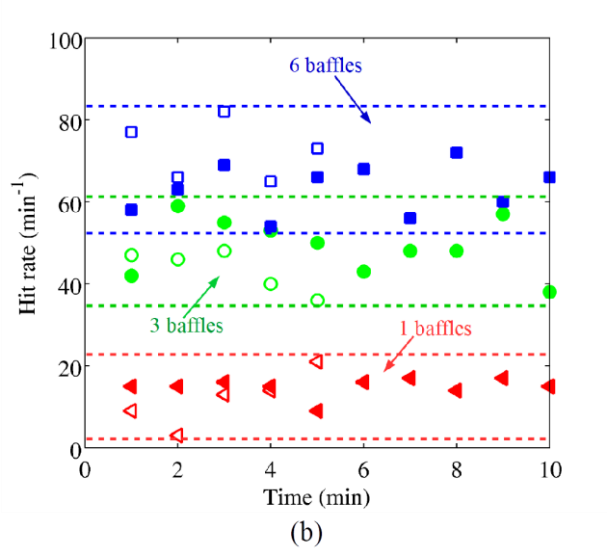

Figure 6: Comparison of hit rates from experiments and simulations: (a) hit rates from three different ray-tracing approaches with various numbers of baffles; (b) hit rates of various numbers of baffles in reflection mode (open markers) and experimental data (closed markers) at each 1 min interval. The dash lines represent the range of the hit rate from simulations and experiments with respect to each number of baffles.

Figure 6 compares the hit rates obtained from the above-mentioned three ray-tracing modes with in-line experiments. For all ray tracing modes, the hit rate increases with increasing number of mixing baffles, while the direct detection modes, including normal and oblique modes, result in higher hit rate than the reflection mode. In this study, small number of tablets and baffles are used in the experiments and simulations. The tablets can roll between baffles without reaching the height of the incoming ray during the pan rotation. A ‘hit’ can only be obtained when the tablet is lifted high enough by the baffle to have an interaction with the incoming ray. Therefore, more baffles lead to a larger probability for a hit. Besides the restriction on the focal length, a successful reflection measurement can only be acquired when the reflected ray hits the receiver. This

significantly decreases the chance to have a hit in the reflection mode. It is worth mentioning that both experiments and simulations can resolve the hit rate at a specific time interval as indicated by Figure 6 which shows that the distribution of hit rates from simulation at each time interval is within the range of experimental data. Nevertheless, it can be seen that the reflection mode agrees well with the experimental data within the range of $\pm 2\sigma$, where σ is the calculated standard deviation. This indicates that the sampling process in reflection mode matches the experimental process. In the following analysis, all ray-traced data are from the reflection mode unless explicitly stated otherwise.

3.2 Spatial distribution of hits from simulations

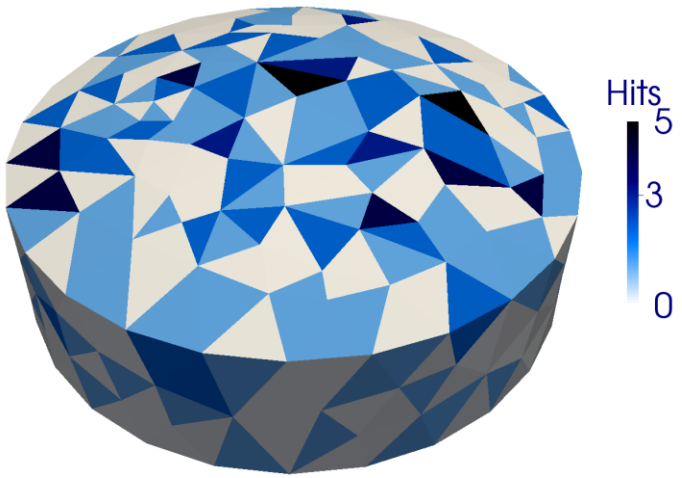

Figure 7: The spatial hit distribution on a representative tablet for the case of 6 baffles accumulated over a duration of 5 min of simulation. When a hit is detected on a specific triangular element on a tablet, the hit will be added onto the triangular element at the same location of the representative tablet which eventually shows the spatial distribution of aggregated hits.

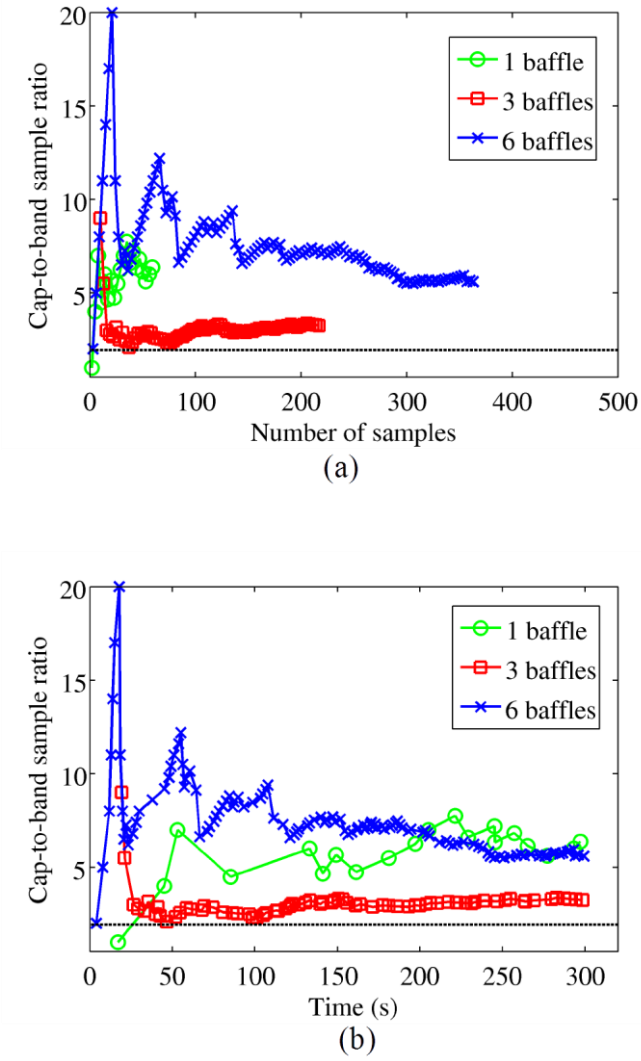

Figure 8: Cap-to-band sample ratios for various number of baffles from the ray-tracing method. (a) Cap-to-band sample ratio against number of samples, and (b) cap-to-band sample ratio against time. The dashed line shows cap-to-band surface area ratio of the tablet. The cap is referred to as the dome-shaped upper and lower surface of the tablet, while the band is the central cylindrical surface of the table.

The numerical model combined with the ray-tracing method provides valuable insights into the origin of the thickness measurement, which cannot be obtained from terahertz in-line experiments alone. As shown in Figure 7, the spatial distribution of hits can be determined within the ray-tracing simulation and aggregated onto a representative tablet over the entire 5 minute simulation time. This information can be used to distinguish between the number of hits from the caps and that from the band. Therefore, the cap-to-band sample ratio, which is the number of hits on caps divided by that on the band, can be calculated from the hit distribution. Figure 8 shows the cap-to-band sample ratio obtained from the ray-tracing method during mixing. The cap-to-band sampling ratio is calculated as the number of hits on the cap divided by the number of hits on the band. Since the hit can occur either on the cap or on the band, at the beginning of the simulation, the cap-to-band sampling ratio fluctuates with the hit location. However, as the numbers of hits on the cap and band accumulate and become large enough (for 3 and 6 baffles), the cap-to-band sampling ratio approaches to an asymptotic value. It is noticeable that the cap-to-band sample ratio varies with the number of baffles. The influence of the number of baffles on the cap-to-band sample ratio does not demonstrate a systematic trend in this study due to a small number of tablets and relatively short measurement time. Nevertheless, the cap-to-band sample ratios with various numbers of baffles are generally higher than the dashed line which represents the cap-to-band surface area ratio. This means in the ray-tracing (simulating the terahertz in-line sensing) process, the caps have a relatively higher chance to be measured than the band. Assuming that the terahertz in-line experiments have the same cap-to-band sampling ratios as the ray-tracing simulations, the cap-to-band sampling ratios should be further corrected to match the cap-to-band surface area ratio to avoid the biased sampling.

3.3 Comparison of ray-traced data with off-line coating thickness measurements

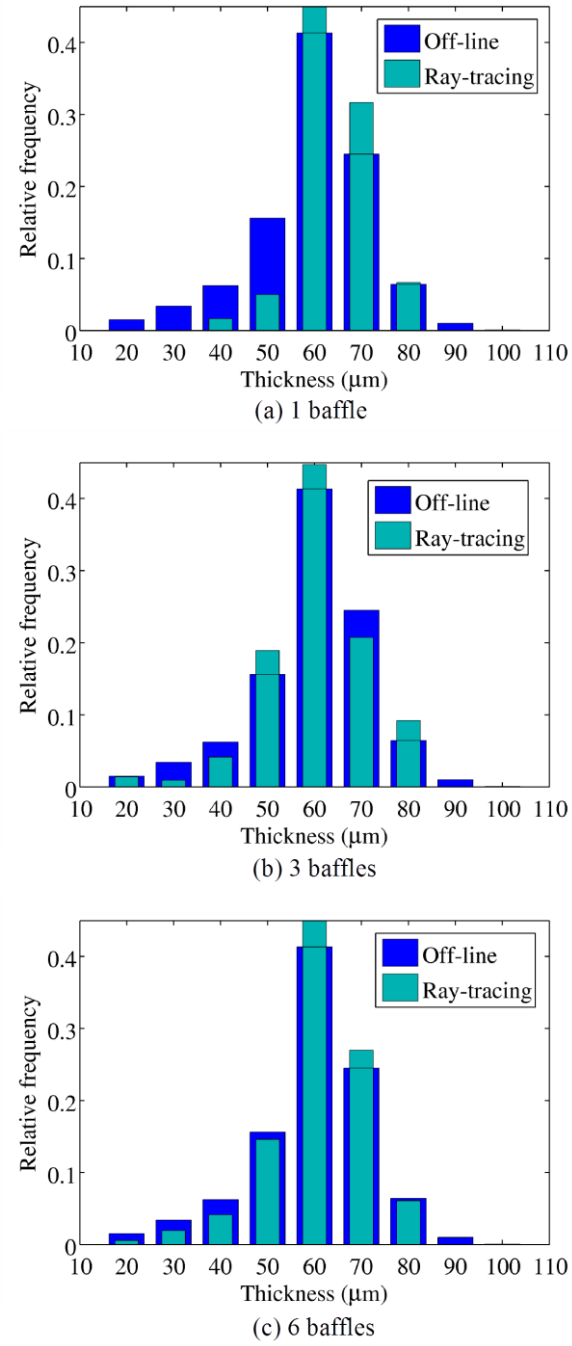

Figure 9: The coating thickness distribution of off-line TPI measurements and of ray-traced data for (a) 1, (b) 3 and (c) 6 baffles. The relative frequency is defined as the number of occurrences (frequencies) in each bar divided by the total number of occurrences.

Figure 9 shows the comparison of the coating thickness distribution between the TPI off-line measurements and ray-traced data with various number of baffles. Using the Anderson-Darling k-sample test (Scholz and Stephens, 1987) for ray-traced data and off-line measurements, p-values are 0.008, 0.3 and 0.06 for 1, 3 and 6 baffles, respectively. For a significance level of 0.05, the ray-traced data from 3 and 6 baffles can match off-line measurements while the ray-traced data from 1 baffle shows statistical difference from off-line measurements. In other words, the match between off-line measurements and ray-traced data becomes better with larger number of baffles. A larger number of baffles leads to a larger number of hits, promotes the mixing of tablets during the process and thus enhances the randomness of sampling (see Appendix B).

3.4 Comparison of ray-traced data with in-line measurements

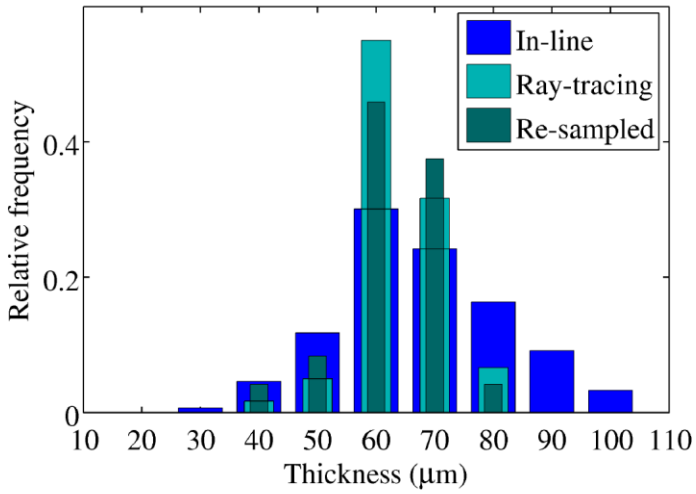

(a) 1 baffle

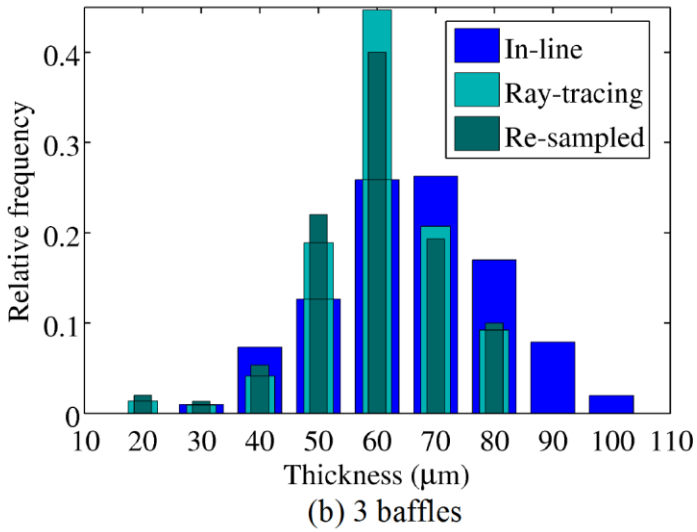

(b) 3 baffles

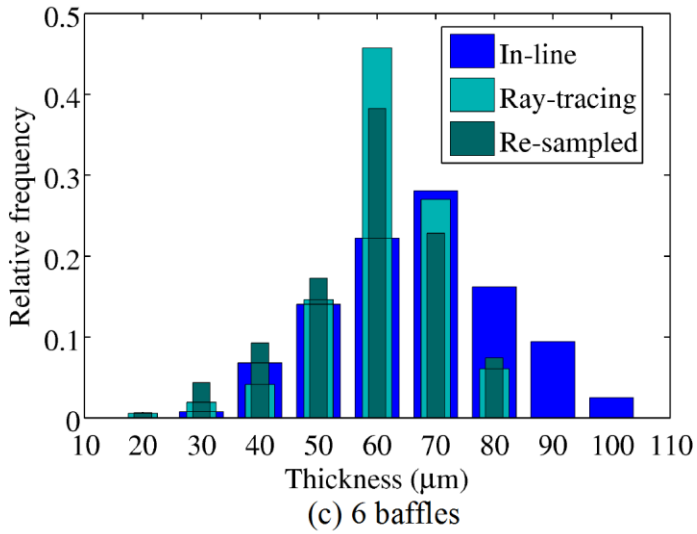

(c) 6 baffles

Figure 10: Coating thickness distribution from terahertz in-line sensing (10 min duration), ray-tracing and re-sampled ray-tracing simulations (5 min duration) with various numbers of baffles. The re-sampled data is the ray-traced data re-sampled to match the cap-to-band sampling ratio to the cap-to-band surface area ratio.

Figure 10 compares the ray-traced data against the results from the terahertz in-line sensing. The coating thickness distributions from simulations and experiments are centred around 60 to 70 μm. However, the ray-traced data have smaller coating thickness down to 20 μm while the in-line measurements contain coating thickness values up to 100 μm. In this study, the ray-traced data is based on the off-line measurements from 24 coated tablets as shown in Figure 9. The mean coating thickness of tablet *i*, $\bar{h}_i$, from off-line TPI measurements can be calculated as:

$$\bar{h}_i = \frac{\sum_{j=1}^{N_i^p} h_i^j}{N_i^p} \tag{2}$$

where h_i^j is the coating thickness of tablet *i* at pixel *j*; N_i^p is the number of pixels from the terahertz image of the tablet *i*. The mean coating thickness of N_t (= 24) tablets is given by

$$\bar{h} = \frac{\sum_{i=1}^{N_t} \bar{h}_i}{N_t} \tag{3}$$

With the mean coating thickness of each tablet, the inter-tablet coating variability, S, can be defined as:

$$S = \frac{\sqrt{\frac{1}{N_t - 1}\sum_{i=1}^{N_t}\left(\bar{h}_i - \bar{h}\right)^2}}{\bar{h}} \tag{4}$$

For each tablet, the intra-tablet coating variability is the relative standard deviation (RSD) to its own mean coating thickness, which can be calculated as:

$$s_i = \frac{\sqrt{\frac{1}{N_i^p - 1}\sum_{j=1}^{N_i^p}\left(h_i^j - \bar{h}_i\right)^2}}{\bar{h}_i} \tag{5}$$

In order to characterise the intra-tablet coating variability of all tablets, a mean intra-tablet coating variability can be defined as:

$$\bar{s} = \frac{\sum_{i=1}^{N_t} \bar{s}_i}{N_t} \tag{6}$$

For both in-line and ray-traced data, the mean coating thickness can be calculated as:

$$\bar{H} = \frac{\sum_{j=1}^{N_I} h^j}{N_I} \tag{7}$$

where h^j is the coating thickness at measurement j; N_I is the total number of in-line or ray-traced measurements. The RSD for in-line measurements can be defined as:

$$\sigma = \frac{\sqrt{\frac{1}{N_I - 1}\sum_{j=1}^{N_I}\left(h^j - \bar{H}\right)^2}}{\bar{H}} \tag{8}$$

Figure 11 shows the mean coating thickness and the RSD of the coating thickness distribution from ray-traced data and in-line measurements during the mixing process. The variations between each minute from simulations and experiments are relatively small during the mixing process. In general, the mean coating thickness and RSD of ray-traced data are smaller (5% - 10%) than those of the corresponding in-line measurements. The ray-traced data with 1 baffle have a slightly larger mean coating thickness and smaller RSD, compared to ray-traced data with 3 and 6 baffles, especially at the beginning of simulations. This is possibly because the ray-tracing data with 1 baffle result in a smaller number of hits, which by chance gives a slight difference as discussed the above section. It also shows that in the last 2 minutes of the process, as the number of hits increases,

the mean coating thickness from ray-traced data with 1 baffle starts to decrease and the RSD increases.

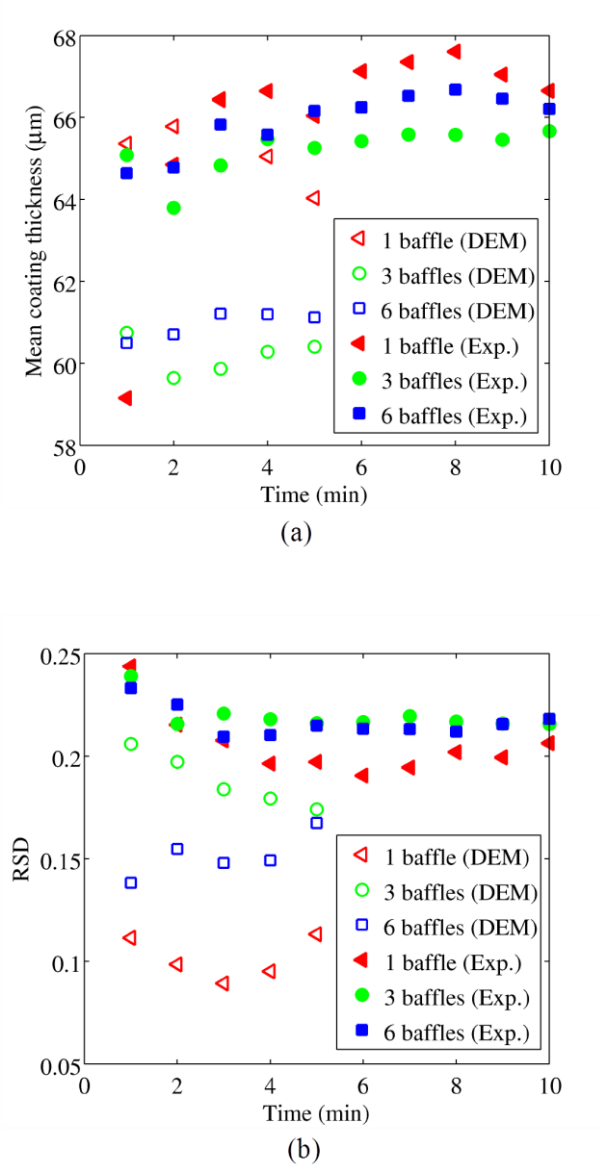

Figure 11: Mean and RSD of coating thickness distribution from ray-traced (open markers) and in-line data (close markers) during mixing. (a) Mean coating thickness, and (b) relative standard deviation of coating thickness distribution. The durations of simulations and experiments are 5 and 10 min, respectively.

The mean thickness, inter- and mean intra-tablet variability from the off-line measurements are 59.1 μm, 0.036 and 0.21, respectively (see Appendix C). The mean thicknesses and RSD of ray-traced data and in-line measurements at the end of simulations and experiments are shown in Table 2. For the mean thickness, the ray-traced data is similar to the off-line measurements since the ray-traced data can represent the off-line measurements as shown in Figure 9. However, the in-line measurement data are slightly higher (4-10%) than the off-line and ray-traced data, which agrees with previous experiments (May et al., 2011). In terahertz in-line measurement, the tablet is moving during the sampling. In order to distinguish the two signal peaks from the reflections on the tablet surface and coating interface as discussed in Section 2 Methodology, it requires a relatively conservative acceptance criteria that the thickness under 30 μm will be considered unreliable and ignored. In addition, the off-line measurements are from a small number of randomly selected tablets (24 tablets), which may cause certain variance between the two sets of data.

In principle, the coating thickness distribution from the in-line experiments is a combined result of the coating thickness difference within each tablet (intra-tablet variability) and across all tablets (inter-tablet variability). However, for these coated tablets, the intra-tablet variability (0.21) is much larger than the inter-tablet variability (0.036) by almost one order of magnitude, which indicates that mean coating thicknesses of off-line tablets are relatively equal. In other words, the intra-tablet coating thickness distribution plays a dominant role in the coating thickness variability of in-line measurements. In in-line measurements, the hits are from different locations (e.g. caps and band) on different tablets as indicated in Figure 7. In other words, since the difference of mean coating thicknesses between tablets are negligible, it can be considered that the variability of the in-line data is mainly the intra-tablet coating thickness distribution within the tablet. Therefore, the

RSD of ray-traced and in-line data is close to the value of intra-tablet variability as shown in Table 2.

Table 2: Mean thicknesses (μm) and RSD of ray-tracing and in-line data. The mean thickness, inter- and mean intra-tablet variability of off-line measurements are 59.1 μm, 0.036 and 0.21.

	1 baffle		3 baffles		6 baffles	
	Mean (μm)	RSD	Mean (μm)	RSD	Mean (μm)	RSD
Ray-tracing	64.0	0.11	60.4	0.17	61.1	0.17
In-line	66.7	0.2	65.6	0.22	66.2	0.22
Corrected ray-tracing	63.5	0.13	59.6	0.19	58.9	0.22
Corrected in-line	66.2	0.24	64.7	0.25	63.8	0.28

As discussed in above sections, the mean coating thickness of in-line measurements is slightly larger than that of off-line and ray-traced data. According to Figure 8, and assuming that the ray-tracing simulations can represent the terahertz in-line experiments, the cap-to-band sample ratio is higher than the cap-to-band surface area ratio in both methods. At the same time, off-line measurements show that the coating thickness (62.4 μm in average) of the cap is higher than that (53.7 μm in average) of the band. The combination of these two situations can cause biased statistical results. In order to correct this, due to the coating thickness difference between the cap and band, the cap-to-band sample ratio should be equal to the cap-to-band surface area ratio. In particular, the ray-traced data from the cap of tablets is randomly re-sampled to ensure that the ratio of the number of re-sampled data from the cap to the number of ray-traced data from the band of tablets is equal to the cap-to-band surface area ratio. The comparisons between the original and

re-sampled ray-traced data are shown in Figure 10. Generally, the re-sampled data become less concentrated in categories of 60 and 70 μm than the original ray-traced data.

In Table 2, each statistics (e.g. mean thickness and RSD) from corrected (re-sampled) ray-traced data are calculated from 6 sets of randomly re-sampled data to minimise possible bias from the re-sampling process. It can be seen that the corrected mean thickness and RSD of the re-sampled data are closer to the off-line measurement. Based on the ratio of corrected statistics of re-sampled data to the statistics of original ray-traced data, the statistics of in-line measurements can also be corrected as:

$$\mu_{ic} = \frac{\mu_{rc}}{\mu_r}\mu_i \tag{9}$$

where μ_i is the original in-line statistics (e.g. mean thickness and RSD); μ_{rc} and μ_r are the corrected statistics of re-sampled ray-traced data and the statistics of original ray-traced data, respectively. As shown in Tables 2, the corrected mean thickness is generally smaller than the original data and closer to the off-line measurement, while the corrected RSD is slightly larger than the original in-line RSD. According to the DEM analysis, the original ray-traced data (in-line measurements) have a larger cap-to-band sampling ratio, which means more hits are from the cap of tablets with a larger coating thickness. This leads to a larger mean coating thickness of the original data than that of resampled data. On the other hand, since the re-sampled data follows the cap-to-band surface area ratio which is smaller than the original cap-to-band sampling ratio, the data become more dispersed over the cap and band, and therefore the RSD of the re-sampled (in-line) data is larger. Nevertheless, this data analysis demonstrates that the DEM and ray-traced data can provide a detailed information to further investigate the terahertz in-line measurements.

The DEM simulation of multi-sphere tablets may show some discrepancy from the actual dynamics of tablets with flat surfaces, especially for the orientation of tablets. Theoretical studies (Höhner et al., 2011) indicate that the temporal force evolution of the multi-sphere model shows some differences from that of the meshed model (polyhedron) during collisions. On the other hand, more recent research (Pasha et al., 2016) have shown that the multi-sphere model can achieve statistical agreement with the experiments in particle mixing/blending. In this paper, the hit rates from simulations match those from experiments. If there is a large discrepancy between simulations and experiments regarding the orientation of tablets, we would expect the hit rate to reflect the discrepancy. Since in this study it does not, we assume that DEM simulations with multi-sphere tablets can very closely approximate the actual tablet dynamics. However, further detailed investigations will be conducted.

In this study, the presented modelling method assumes a perfect specular reflection from encountered tablets, which does not rely on material properties. Thus, it is generally applicable for modelling the sampling mechanism of calibration-free process analytical technologies such as TPI and OCT. The uniqueness of TPI is that the terahertz radiation can penetrate through polymer-based coatings and is insensitive to pigments that would otherwise hinder optical-based techniques such as OCT (Brock et al., 2013a, 2013b; Ho et al., 2007; Lin et al., 2017; Shen, 2011). For actual coating processes, the water moisture in the coating can attenuate the terahertz energy and cause a weaker reflection. However, the extent of attenuation ultimately depends on the amount and distribution of water moisture in the coating as a TPI measurement would average it out over the terahertz spot size (approximately 200 μm in this study). Under a well-controlled coating process, the effect of water moisture is expected to be small enough so that the signal can still be detected following appropriate signals processing. As a matter of fact, TPI has been demonstrated that in

realistic coating experiments, good agreements between in-line and off-line measurements were observed (May, et al., 2011; Lin et al., 2017).

4. Conclusions

In this study, terahertz in-line sensing was employed to measure the coating thickness distribution during the mixing process of pharmaceutical film-coated tablets in a rotating pan. DEM combined with a ray-tracing approach was used to model and analyse the in-line coating thickness measurements.

The reflection mode of the ray-tracing method was able to quantitatively predict the hit rate in experiments, which increased with an increasing number of baffles in the coating drum for the geometries used in this study.

The coating thickness distribution from the ray-tracing method was found to be in a good agreement with the off-line coating thickness measurements. The mean coating thickness from the terahertz in-line measurements was 4-10% larger than that of ray-traced data. As the inter-tablet coating thickness variability was relatively low in this work, the relative standard deviation from the ray-tracing method and terahertz in-line experiments represents the intra-tablet coating thickness variability.

The ray-tracing method can also be used to further explore the cap-to-band sample ratio, which can be combined with the cap-to-band surface area ratio to correct the ray-traced and in-line measurements. The corrected mean thicknesses of ray-traced and in-line data were closer to the off-line measurements than original data, while the corrected RSDs of ray-traced and in-line data were slightly larger than original data.

This study has demonstrated how discrete element method can be combined with the ray-tracing method in order to model and explain the terahertz in-line measurement of a pharmaceutical process. Whilst terahertz in-line sensing was used in this work, without a loss of generality, other in-line measurement modalities combined with these numerical models could provide fundamental understanding to future industrial process control.

Acknowledgments

The authors acknowledge the financial support from UK Engineering and Physical Sciences Research Council Research Grant EP/L019787/1, EP/L019922/1 and EP/R019460/1. The authors acknowledge the staff of the electronics and mechanical workshops in the Department of Chemical Engineering and Biotechnology at University of Cambridge. HL also acknowledges travel support from Joy Welch Educational Charitable Trust. Additional supporting data related to this publication is available from the University of Cambridge data repository (https://doi.org/10.17863/CAM.24700).

Appendix A

As introduced in the Methodology section, at some areas (of caps and band), the surface of the constitute sphere is higher than the meshed surface area. In addition, the surface of the drum is divided into triangular elements. Both of these setups will lead to a relatively larger normal distance between the meshed tablet and the curved drum surface. For instance, after the position and orientation of meshed tablets are mapped from multi-spheres, there is usually a distance between the meshed tablet and drum surface, such as when the multi-sphere is laying on the drum

surface. This distance will be added to the normal distance between the meshed tablet and terahertz sensor when there is a hit. In other words, when there is a hit, the normal distance between the meshed tablet and terahertz sensor in modelling is usually larger than the focal range (e.g. 7 ± 0.5 mm) which is corresponding to the Rayleigh range of the optics in experiments.

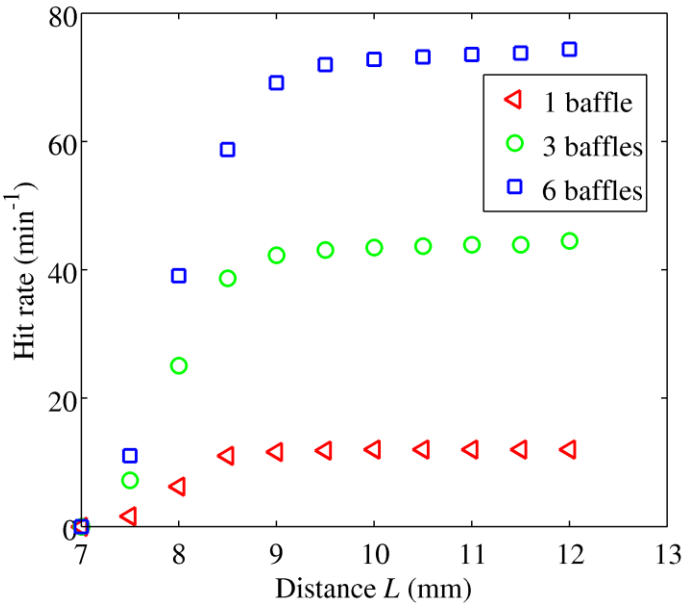

Figure A.1: The variation of hit rate against the normal distance (L).

Figure A.1 shows the variation of hit rate against the normal distance limit between the meshed tablet and terahertz sensor in ray-tracing simulations. For all numbers of baffles, the hit rate increases when a larger normal distance (focal length) limit is chosen for the ray-tracing simulation. At about 9 mm, the hit rate becomes stable. As discussed above, the normal distance between the meshed tablet and terahertz sensor in modelling is usually larger than the focal range in experiments. In order to compare the modelling against experimental measurements, a larger

limit of 10 mm (> 9 mm) is chosen. As shown in Figure 6, the hit rate from modelling data agrees with the experimental data. On the other hand, this also indicates that the normal distance between the meshed tablet and terahertz sensor in modelling is generally larger than the focus length in experiments by 1 – 2 mm.

Appendix B

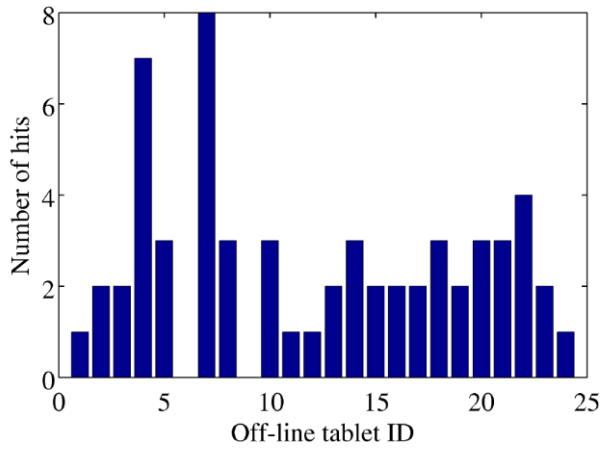

(a)

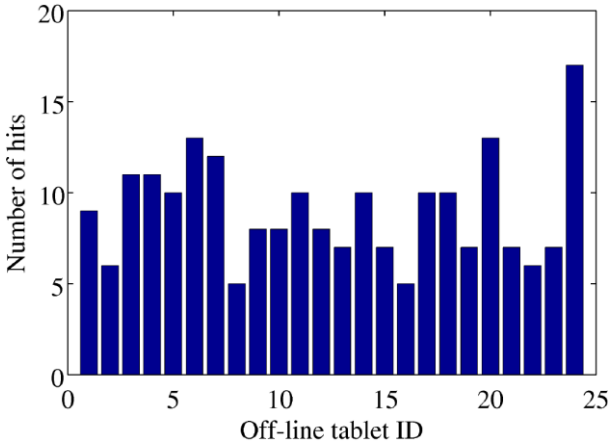

(b)

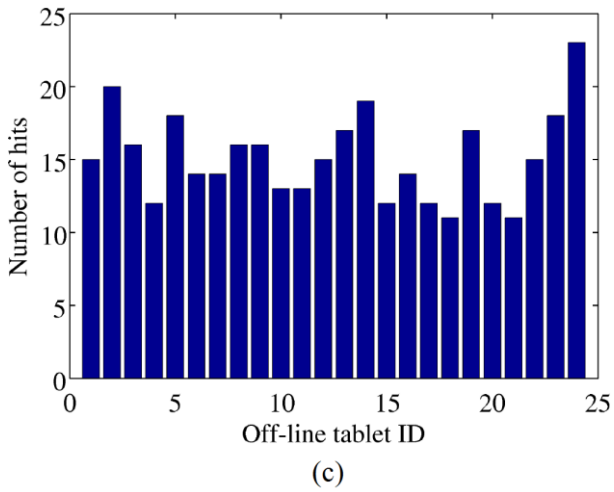

(c)

Figure B.1: The distribution of detected off-line measured tablets in ray-tracing simulations with various baffles: (a) 1 baffle, (b) 3 baffles and (c) 6 baffles. A chi-squared test for randomness shows the p-values are 0.12, 0.57 and 0.93 for 1, 3 and 6 baffles, respectively, which are larger than the significance level (i.e. 0.05).

Due to the relatively large number of tablets in the drum, in this study, it is not realistic to measure the coating thickness distribution of the entire tablet population in an off-line configuration. Therefore, 24 tablets measured off-line are mapped to every 24 DEM tablets until the total 230 tablets are mapped. The randomness of the detection over the 24 off-line tablets, which can be considered as the population of DEM and ray-tracing simulations, can influence the detected coating thickness distribution. The ray-tracing method is able to distinguish which assigned off-line tablet the intersected tablet belongs to. Figure B.1 shows the frequency at which the 24 tablets measured off-line were actually detected from a population of 230 tablets by ray-tracing. For one baffle, the total number of hits is smaller than those from larger numbers of baffles (i.e. 3 and 6) in 5 min simulations, as the hit rate decreases with smaller number of baffles. Even though, almost

all 24 off-line tablets are detected with one baffle, while with larger number of baffles (e.g. 3 and 6), all 24 off-line tablets are got hit. As a further assessment on randomness using the chi-squared test, p-values for all cases, which resulted in values of 0.12, 0.57 and 0.93 for 1, 3 and 6 baffles, are larger than the significance level (i.e. 0.05). This indicates the tablet mixing process in the coating pan can be considered as random. Clearly, a larger number of baffles leads to a larger p-value and a better mixing process, which allows the ray-tracing process to obtain a coating thickness distribution closer to the population (off-line data) as shown in Figure 9. It should be noted that these results are obtained from a lab scale setup and the terahertz sensor is located perpendicular to the centre of the coating pan at the horizontal position ($D_e/2$). For an industrial process, a larger coating pan can lead to a different mixing regime especially when baffles with complex shapes are involved. Nevertheless, this study demonstrated that, with appropriate modelling and experimental setup, the DEM combined with the ray-tracing method is capable of capturing the population of coating thickness distribution.

Appendix C

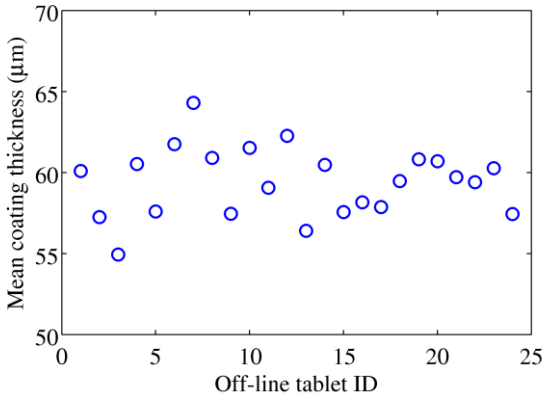

Figure C.1: The mean coating thicknesses of 24 off-line measured tablets.

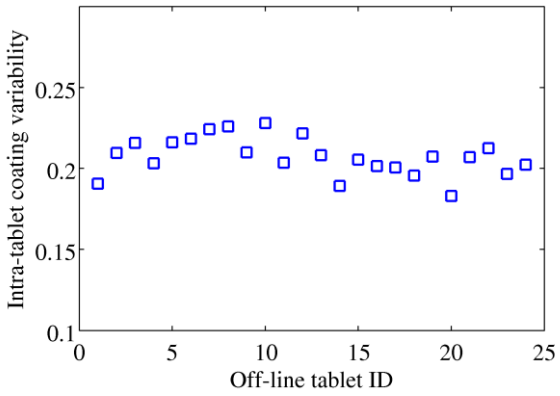

Figure C.2: The intra-tablet coating variabilities of 24 off-line measured tablets.

Figure C.1 shows the mean coating thicknesses of 24 off-line measured tablets. The mean value of the 24 mean coating thicknesses is 59.1 μm. The relative standard deviation of the mean coating thicknesses, which is defined as the inter-tablet coating variability, is 0.036. Figure C.2 shows the intra-tablet coating variabilities of 24 off-line measured tablets. The intra-tablet coating variability of each tablet is calculated by Eq. (5) from the coating thicknesses on triangles as shown in Figure 4. The mean intra-tablet coating variability of 24 tablets is 0.21. In this study, the intra-tablet variability is generally larger than the inter-tablet variability.

References

Boehling, P., Toschkoff, G., Knop, K., Kleinebudde, P., Just, S., Funke, A., Rehbaum, H., Khinast, J.G., 2016. Analysis of large-scale tablet coating: Modeling, simulation and experiments. Eur. J. Pharm. Sci. 90, 14–24. doi:10.1016/j.ejps.2015.12.022

Brock, D., Zeitler, J.A., Funke, A., Knop, K., Kleinebudde, P., 2013a. Evaluation of critical process parameters for intra-tablet coating uniformity using terahertz pulsed imaging. Eur. J. Pharm. Biopharm. 85, 1122–1129. doi:10.1016/j.ejpb.2013.07.004

Brock, D., Zeitler, J.A., Funke, A., Knop, K., Kleinebudde, P., 2013b. Evaluation of critical process parameters for inter-tablet coating uniformity of active-coated GITS using Terahertz Pulsed Imaging. Eur. J. Pharm. Biopharm. 85, 1122–1129. doi:10.1016/j.ejpb.2013.07.004

Di Renzo, A., Di Maio, F.P., 2004. Comparison of contact-force models for the simulation of collisions in DEM-based granular flow codes. Chem. Eng. Sci. 59, 525–541.

Freireich, B., Wassgren, C., 2010. Intra-particle coating variability: Analysis and Monte-Carlo simulations. Chem. Eng. Sci. 65, 1117–1124. doi:10.1016/j.ces.2009.09.066

Freireich, B., Kumar, R., Ketterhagen, W., Su, K., Wassgren, C., Zeitler, J.A., 2015. Comparisons of intra-tablet coating variability using DEM simulations, asymptotic limit models, and experiments. Chem. Eng. Sci. 131, 197–212. doi:10.1016/j.ces.2015.03.013

Haaser, M., Gordon, K.C., Strachan, C.J., Rades, T., 2013. Terahertz pulsed imaging as an advanced characterisation tool for film coatings — A review. Int. J. Pharm. 457, 510–520. doi:10.1016/j.ijpharm.2013.03.053

Hancock, B.C., Mojica, N., John, -Green K St, Elliott, J. a., Bharadwaj, R., 2010. An investigation into the kinetic (sliding) friction of some tablets and capsules. Int. J. Pharm. 384, 39–45. doi:10.1016/j.ijpharm.2009.09.038

Ho, L., Müller, R., Römer, M., Gordon, K.C., Heinämäki, J., Kleinebudde, P., Pepper, M., Rades, T., Shen, Y.C., Strachan, C.J., Taday, P.F., Zeitler, J. a., 2007. Analysis of sustained-release

tablet film coats using terahertz pulsed imaging. J. Control. Release 119, 253–261. doi:10.1016/j.jconrel.2007.03.011

Höhner, D., Wirtz, S., Kruggel-Emden, H., Scherer, V., 2011. Comparison of the multi-sphere and polyhedral approach to simulate non-spherical particles within the discrete element method: Influence on temporal force evolution for multiple contacts. Powder Technol. 208, 643-656.

Ketterhagen, W.R., 2011. Modeling the motion and orientation of various pharmaceutical tablet shapes in a film coating pan using DEM. Int. J. Pharm. 409, 137–149. doi:10.1016/j.ijpharm.2011.02.045

Kloss, C., Goniva, C., Hager, A., Amberger, S., Pirker, S., 2012. Models , algorithms and validation for opensource DEM and CFD-DEM. Prog. Comput. Fluid Dyn. 12, 140–152. doi:10.1504/PCFD.2012.047457

Lin, H., Dong, Y., Markl, D., Zhang, Z., Shen, Y., Zeitler, J.A., 2017. Pharmaceutical Film Coating Catalog for Spectral Domain Optical Coherence Tomography. J. Pharm. Sci. 106, 3171–3176. doi:10.1016/j.xphs.2017.05.032

Lin, H., Dong, Y., Markl, D., Williams, B.M., Zheng, Y., Shen, Y., Zeitler, J.A., 2017. Measurement of the Intertablet Coating Uniformity of a Pharmaceutical Pan Coating Process With Combined Terahertz and Optical Coherence Tomography In-Line Sensing. J. Pharm. Sci. 106, 1075–1084. doi:10.1016/j.xphs.2016.12.012

Lin, H., Dong, Y., Shen, Y., Zeitler, J.A., 2015a. Quantifying Pharmaceutical Film Coating with Optical Coherence Tomography and Terahertz Pulsed Imaging: An Evaluation. J. Pharm. Sci. 104, 3377–3385. doi:10.1002/jps.24535

Lin, H., May, R.K., Evans, M.J., Zhong, S., Gladden, L.F., Shen, Y., Zeitler, J.A., 2015b. Impact of Processing Conditions on Inter-tablet Coating Thickness Variations Measured by Terahertz In-Line Sensing. J. Pharm. Sci. 104, 2513–2522. doi:10.1002/jps.24503

Markl, D., Hannesschlager, G., Sacher, S., Leitner, M., Buchsbaum, A., Pescod, R., Baele, T., Khinast, J.G., 2015. In-Line Monitoring of a Pharmaceutical Pan Coating Process by Optical Coherence Tomography. J. Pharm. Sci. 104, 2531–2540. doi:10.1002/jps.24531

May, R.K., Evans, M.J., Zhong, S., Warr, I., Gladden, L.F., Shen, Y., Zeitler, J.A., 2011. Terahertz in-line sensor for direct coating thickness measurement of individual tablets during film coating in real-time. J. Pharm. Sci. 100, 1535–1544. doi:10.1002/jps.22359

Moes, J.J., Ruijken, M.M., Gout, E., Frijlink, H.W., Ugwoke, M.I., 2008. Application of process analytical technology in tablet process development using NIR spectroscopy: Blend uniformity, content uniformity and coating thickness measurements. Int. J. Pharm. 357, 108–118. doi:10.1016/j.ijpharm.2008.01.062

Möltgen, C. V., Puchert, T., Menezes, J.C., Lochmann, D., Reich, G., 2012. A novel in-line NIR spectroscopy application for the monitoring of tablet film coating in an industrial scale process. Talanta 92, 26–37. doi:10.1016/j.talanta.2011.12.034

Pasha, M., Hare, C., Ghadiri, M., Gunadi, A., Piccione, P.M., 2016. Effect of particle shape on flow in discrete element method simulation of a rotary batch seed coater. Powder Technol. 296, 29-36.

Pei, C., Elliott, J.A., 2017. Asymptotic limits on tablet coating variability based on cap-to-band thickness distributions: A discrete element model (DEM) study. Chem. Eng. Sci. 172, 286–296. doi:10.1016/j.ces.2017.06.029

Pei, C., Wu, C.Y., Adams, M., 2015. Numerical analysis of contact electrification of non-spherical particles in a rotating drum. Powder Technol. 285, 110–122. doi:10.1016/j.powtec.2015.05.050

Pérez-Ramos, J.D., Findlay, W.P., Peck, G., Morris, K.R., 2005. Quantitative analysis of film coating in a pan coater based on in-line sensor measurements. AAPS PharmSciTech 6, E127–E136. doi:10.1208/pt060120

Russe, I.-S., Brock, D., Knop, K., Kleinebudde, P., Zeitler, J.A., 2012. Validation of Terahertz coating thickness measurements using X-ray microtomography. Mol. Pharm. 9, 3551–9. doi:10.1021/mp300383y

Scholz, F.W., Stephens, M.A., 1987. K-Sample Anderson-Darling Tests K-Sample Anderson-Darling Tests. J. Am. Stat. Assoc. 82, 918–924.

Shen, Y.C., 2011. Terahertz pulsed spectroscopy and imaging for pharmaceutical applications: A review. Int. J. Pharm. 417, 48–60. doi:10.1016/j.ijpharm.2011.01.012

Shen, Y.C., Taday, P.F., 2008. Development and application of terahertz pulsed imaging for nondestructive inspection of pharmaceutical tablet. IEEE J. Sel. Top. Quantum Electron. 14, 407–415. doi:10.1109/JSTQE.2007.911309

Suzzi, D., Toschkoff, G., Radl, S., Machold, D., Fraser, S.D., Glasser, B.J., Khinast, J.G., 2012. DEM simulation of continuous tablet coating: Effects of tablet shape and fill level on inter-tablet coating variability. Chem. Eng. Sci. 69, 107–121. doi:10.1016/j.ces.2011.10.009

Toschkoff, G., Just, S., Funke, A., Djuric, D., Knop, K., Kleinebudde, P., Scharrer, G., Khinast, J.G., 2013. Spray models for discrete element simulations of particle coating processes.

Chem. Eng. Sci. 101, 603–614. doi:10.1016/j.ces.2013.06.051

Toschkoff, G., Just, S., Knop, K., Kleinebudde, P., Funke, A., Djuric, D., Scharrer, G., Khinast, J.G., 2015. Modeling of an Active Tablet Coating Process. J. Pharm. Sci. 104, 4082–4092. doi:10.1002/jps.24621

Turton, R., 2008. Challenges in the modeling and prediction of coating of pharmaceutical dosage forms. Powder Technol. 181, 186–194. doi:10.1016/j.powtec.2006.12.006

Wirges, M., Funke, A., Serno, P., Knop, K., Kleinebudde, P., 2013. Development and in-line validation of a Process Analytical Technology to facilitate the scale up of coating processes. J. Pharm. Biomed. Anal. 78–79, 57–64. doi:10.1016/j.jpba.2013.01.037